

Correlation in Molecular Models
Many-body Potentials and Frustration

Embracing Stochasticity in Electrochemical Modeling

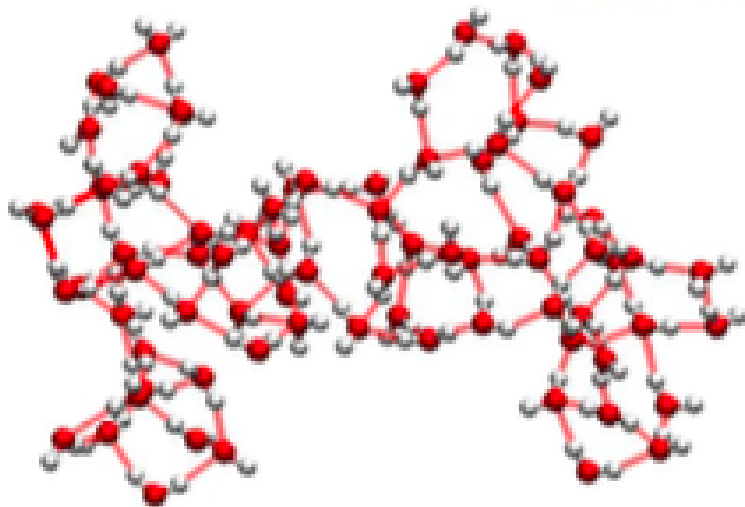
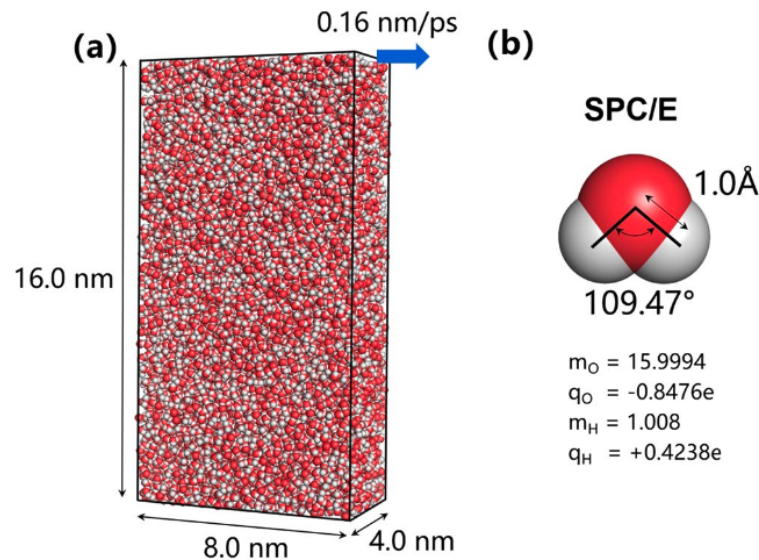
IPAM

Sept 15, 2025

Keith Promislow



Water forms Networks



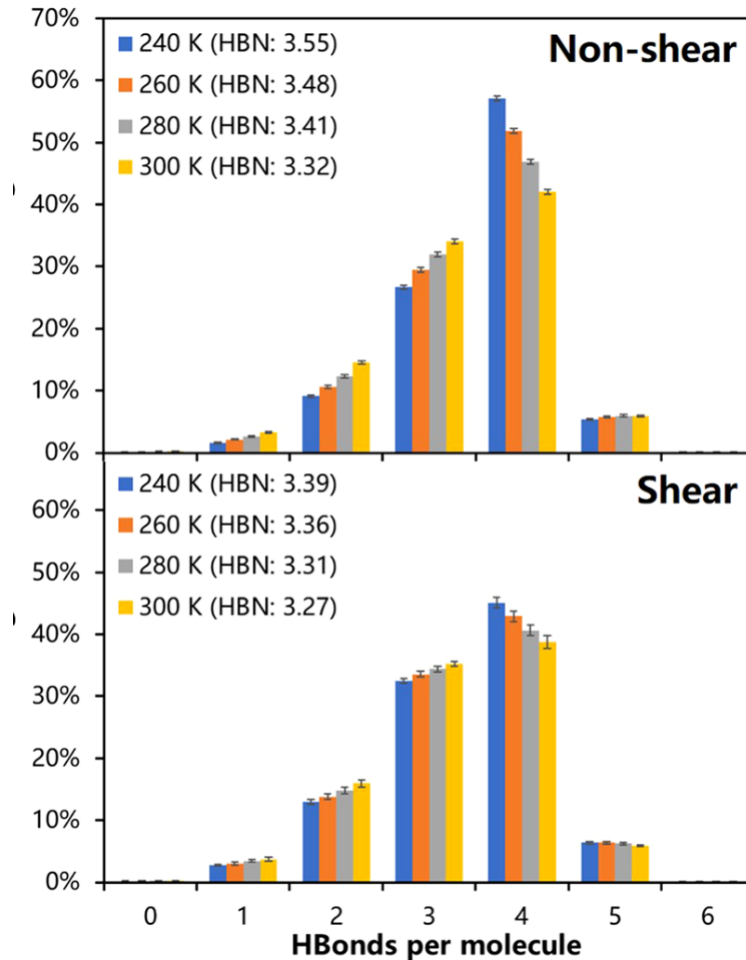
Highly polar solvent with tetrahedral shape

Strong dipole moment

Forms random networks of hydrogen bonds. Data is from molecular dynamics using distance/angle metrics to infer hydrogen bonding.

Goa, Fang, Ni, Scientific Reports 2021

Water is Exceptional



Anomalous properties:

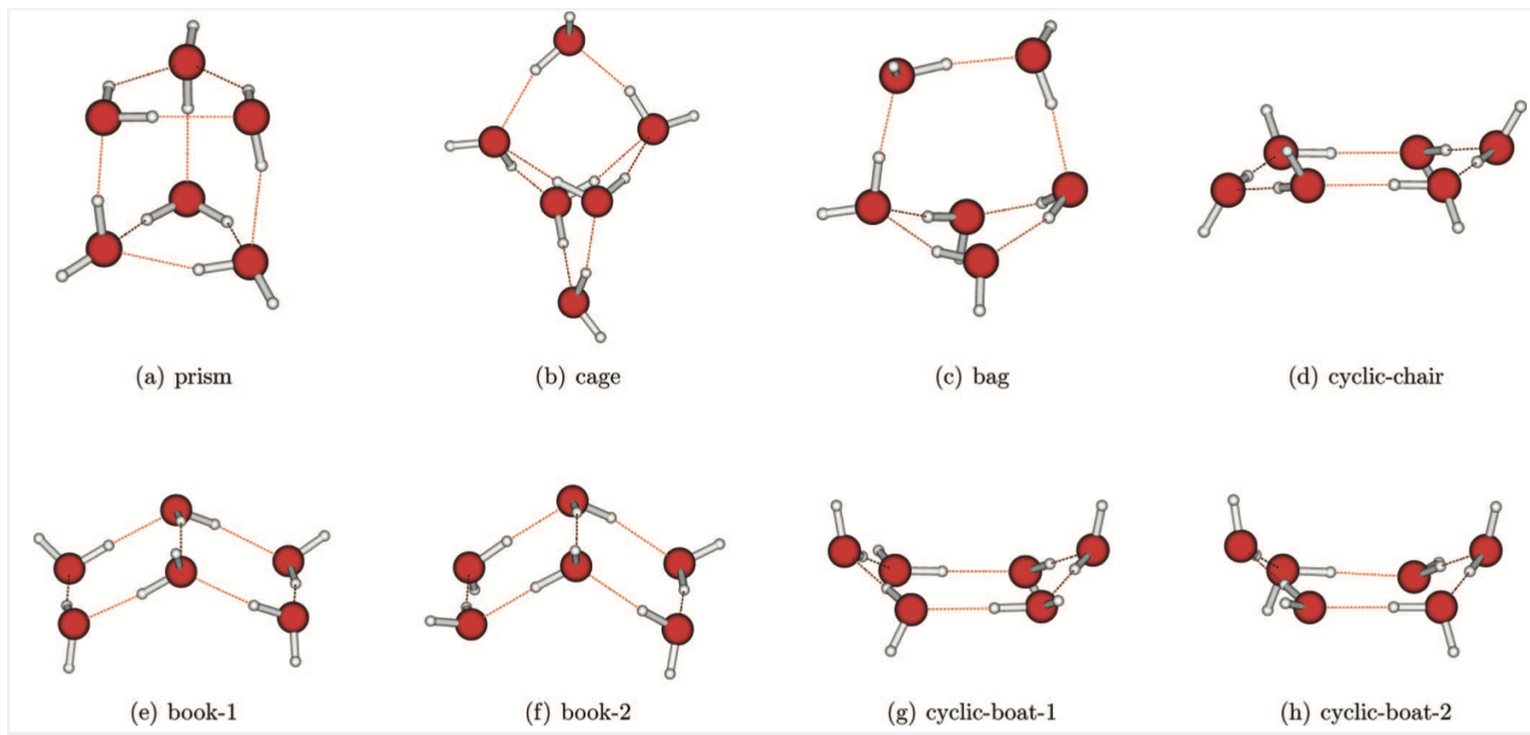
- + Density maximum at 4°C,
- + Steep increase in isothermal compressibility and heat capacity upon cooling

- + Non-Arrhenius behavior of viscosity and diffusivity at low pressure

Wide distribution of hydrogen bond statistics, relatively insensitive to temperature or shear.

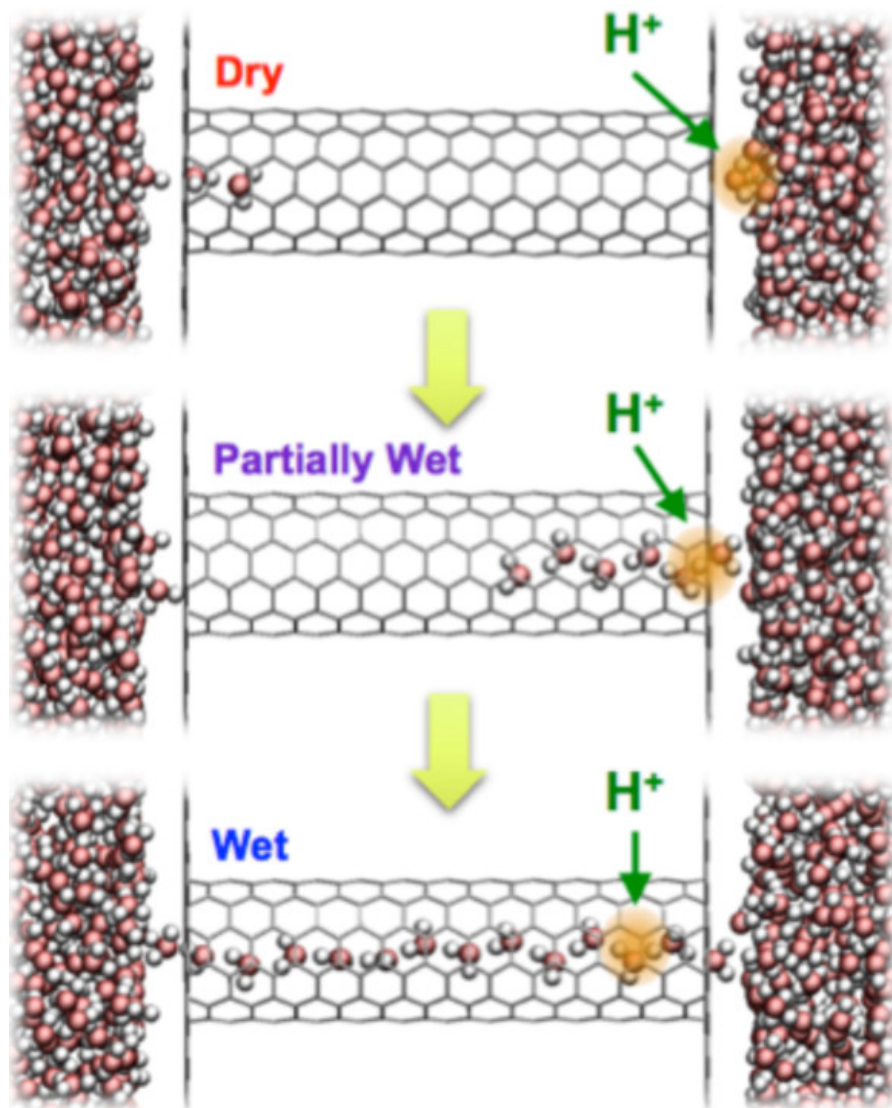
Goa, Fang, Ni, Scientific Reports
2021

Water Clusters



Classic 6-body water clusters, from Bates & Tschumper **J. Phys. Chem. A** (2009).

Frustration and Water Wires

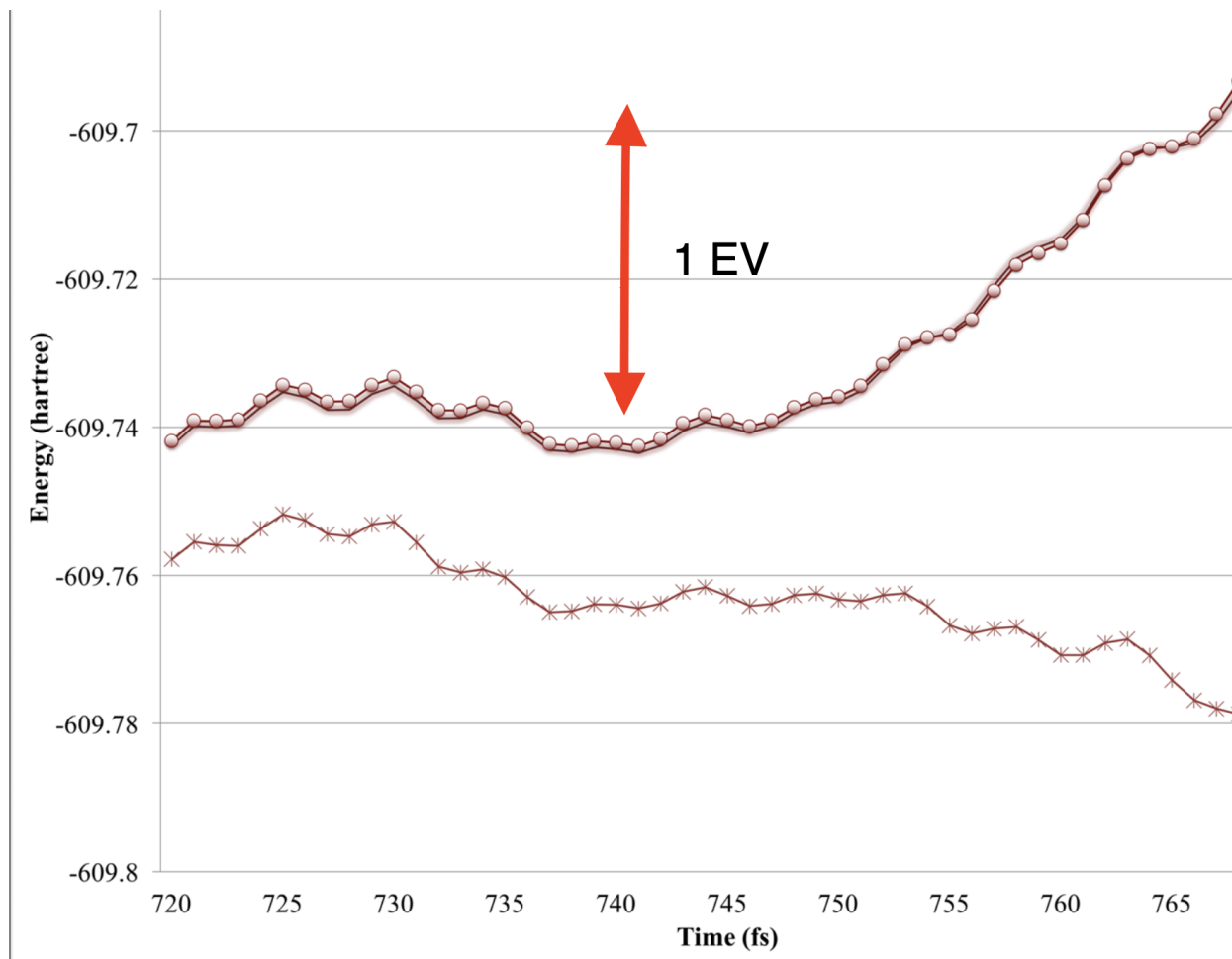


Water molecules induced to form a “water wire” within a narrow hydrophobic cylinder. The wetted cylinder is able to conduct a proton, modeling a proton channel.

Key issue, the anomalously “long-tailed” distribution of hydrogen bond count. Roughly 15% of water molecules have two or fewer hydrogen bonds. These misfits/defects will enter into the hydrophobic tube.

Greg Voth et al, J. Phys. Chem. B 2015

Many-body Interactions

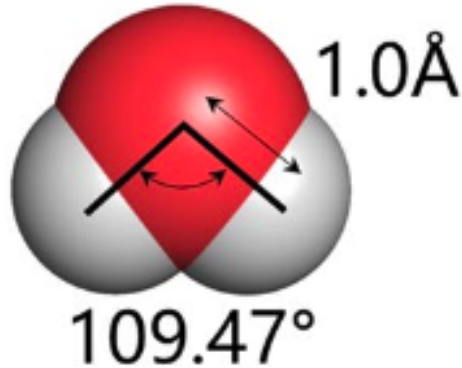


“It has been demonstrated that three-body effects play an integral role in systems dominated by quantum many-body effects, in particular in water clusters.” Pruitt et al **J. Chem. Theor. Comp.** (2016)

Stochastic Fluctuations in Water Potential



Continuum Models from Polar Solvent: Stockmeyer Model



$$m_O = 15.9994$$

$$q_O = -0.8476e$$

$$m_H = 1.008$$

$$q_H = +0.4238e$$

Fix a domain $\Omega \subset \mathbb{R}^2$. Consider N interchangeable agents with locations $x_i \in \Omega$ and introduce the dipole charge locations

$$x_i^\pm = x_i \pm \frac{\ell}{2} d(\theta)$$

where the dipole angle vector

$$d(\theta) = \begin{pmatrix} \cos \theta \\ \sin \theta \end{pmatrix},$$

controls orientation. The partial charge at x_i^\pm is $\pm q$.

The empirical charge density is

$$q_N = q \sum_{i=1}^N \left(\delta_{x_i^+} - \delta_{x_i^-} \right).$$

The electric potential solves Poisson's equation

$$\epsilon_0 \Delta \psi = q_N.$$

If G is the periodic Greens function for the Laplacian on Ω . We make the approximation

$$G(x - x_i^+) - G(x - x_i^-) \approx \ell \nabla G(x - x_i) \cdot d(\theta_i),$$

under which the electric potential becomes

$$\psi = \frac{q\ell}{\epsilon_0} \sum_{i=1}^N \nabla_x G(x - x_i) \cdot d(\theta_i),$$

and the electric potential energy

$$\mathcal{E}_E(X, \Theta) = \frac{q^2 \ell^2}{\epsilon_0} \sum_i^N \sum_{j \neq i}^N d(\theta_j) \nabla_x^2 G(r_{ij}) d(\theta_i),$$

Here ∇^2 denotes the Hessian operator and

$$r_{ij} := x_i - x_j$$

is interparticle distance vector.

Caveat: Short Range Forces

Collisions are guided by electronic interactions via a short-range potential $\Phi = \Phi(\boldsymbol{r}, \boldsymbol{\theta})$ where \boldsymbol{r} is a distance and $\boldsymbol{\theta}$ is a relative angle. A simple model, borrowing from collision operators

$$\Phi(\boldsymbol{r}, \boldsymbol{\theta}) = \left(\frac{1}{r^\alpha} - b(\boldsymbol{\theta}) \right) e^{-r^2},$$

which is of Lennard-Jones type in \boldsymbol{r} . The angular dependence should favor misalignment, $\boldsymbol{\theta} = \pi$, pushing the location of the minima further out and reduces the depth of the minima, for example

$$b(\boldsymbol{\theta}) = (1 - \cos(\boldsymbol{\theta}))^2/4.$$

The short range collision potential takes the form

$$\mathcal{E}_\Phi := \sum_i^N \sum_{j \neq i}^N \Phi(|\boldsymbol{r}_{ij}|, \boldsymbol{\theta}_i - \boldsymbol{\theta}_j).$$

Dipolar Molecules the Hamiltonian

We introduce a Hamiltonian of kinetic and potential energies written in terms of position and momentum

$$\mathcal{H}(X, \Theta, P, Q) = \mathcal{U}_E(X, \Theta) + \mathcal{U}_\Phi(X, \Theta) + \sum_i \left(\frac{|p_i|^2}{2m} + \frac{q_i^2}{2I} \right),$$

where $p_i = v_i m$ is the linear momentum $q_i = I\omega_i$ is its angular momentum, crucially

$$I = m\ell^2/4 \ll m$$

The model is partially motivated by the approach of

G. Monet, F. Bresme, A. Kornyshev, H. Berthoumieux, Nonlocal dielectric response of water in nanoconfinement, *Physical Review Letters* **126** 216001 (2021).

Subject to the substitution $d(\theta) \leftrightarrow m$ (polarization field).

The N -particle Hamiltonian ODE

$$\dot{x}_i = p_i/m = v_i,$$

$$\dot{\theta}_i = q_i/I = \omega_i,$$

$$m\dot{v}_i = -\frac{q^2\ell^2}{\epsilon_0} \sum_{j \neq i}^N d(\theta_j) \nabla^3 G(r_{ij}) d(\theta_i) - \sum_{j \neq i}^N \partial_r \Phi(|r_{ij}|, \theta_i - \theta_j) r_{ij},$$

$$I\dot{\omega}_i = -\frac{q^2\ell^2}{\epsilon_0} \sum_{j \neq i}^N d(\theta_j) \nabla^2 G(r_{ij}) d^\perp(\theta_i) - \sum_{j \neq i}^N \partial_\theta \Phi(|r_{ij}|, \theta_i - \theta_j),$$

Here \perp denotes rotation by $\pi/2$ in particular $\partial_\theta d(\theta) = d^\perp(\theta)$.

We record the force fields

$$F^x(z_i, z_j) := -\frac{q^2\ell^2}{m\epsilon_0} d(\theta_i) \nabla_x^3 G(x_i - x_j) d(\theta_j),$$

$$F^\theta(z_i, z_j) := -\frac{q^2}{m\epsilon_0} d(\theta_i) \nabla_x^2 G(x_i - x_j) d(\theta_j).$$

BBGKY Heirachy

The dipole model is a two-body interaction. If $f_N(Z_1, \dots, Z_N)$ is the N -particle probability distribution, taking marginals The one-marginal evolution couples to the two-marginal

$$\begin{aligned} \partial_t f_{N,1} + v_1 \cdot \nabla_{x_1} f_{N,1} + \omega \partial_\theta f_{N,1} + \\ (N-1) \left(\nabla_{v_1} \cdot (F^x \circledast_{12} f_{N,2}) + \nabla_{\omega_i} (F^\theta \circledast_{12} f_{N,2}) \right) = 0. \end{aligned}$$

Here we introduced the two-point convolution.

If $F : \mathbb{R}^{2d} \mapsto \mathbb{R}$ and $f_K : \mathbb{R}^{2dK} \mapsto \mathbb{R}$

$$(F \circledast_{ij} f_K)(z_i) := \int_{\mathbb{R}^{2(d-1)K}} F(z_i - z_j) f_K(z_1, \dots, z_K) \overbrace{dz_1 \dots dz_K}^{dz_i \notin}.$$

In the mean-field limit $f_{N,k} \rightarrow f^{\otimes k}$ and the BBGKY reduces to a Vlasov system

$$f_t + v \nabla_x f + \omega \partial_\theta f + \nabla_v \cdot ((\bar{F}^x * f) f) + \partial_\omega ((\bar{F}^\theta * f) f) = 0.$$

Mean field and Continuum Quantities

Identify the microscopic variables $\tilde{\mathbf{z}} = (\mathbf{v}, \boldsymbol{\theta}, \boldsymbol{\omega})$ and define the local density

$$\rho(t, \mathbf{x}) := \int_{\mathbb{R}^4} f(t, \mathbf{x}, \tilde{\mathbf{z}}) d\tilde{\mathbf{z}},$$

the density-weighted macroscopic velocity

$$\rho(t, \mathbf{x}) \mathbf{U}(t, \mathbf{x}) := \int_{\mathbb{R}^4} \mathbf{v} f(t, \mathbf{x}, \tilde{\mathbf{z}}) d\tilde{\mathbf{z}},$$

the density-weighted displacement field \mathbf{D}

$$\rho(t, \mathbf{x}) \mathbf{D}(t, \mathbf{x}) := \int_{\mathbb{R}^4} d(\boldsymbol{\theta}) f(t, \mathbf{x}, \tilde{\mathbf{z}}) d\tilde{\mathbf{z}},$$

and the density-weight macroscopic dipole angular velocity

$$\rho(t, \mathbf{x}) \boldsymbol{\Omega}(t, \mathbf{x}) := \int_{\mathbb{R}^4} \boldsymbol{\omega} f(t, \mathbf{x}, \tilde{\mathbf{z}}) d\tilde{\mathbf{z}}.$$

Hydrodynamic Limit from Vlasov

The Vlasov hydrodynamic limit is given by the projection of the Vlasov system against the functions $\{1, v, d(\theta), \omega\}$ over the microscopic $\tilde{\mathbf{z}}$ variables.

$$\begin{aligned}\partial_t \rho + \nabla_x \cdot (\rho U) &= 0, \\ \partial_t(\rho U) + \nabla_x \cdot (\rho U \otimes U + P^{vv}) &= \frac{\ell^2}{\epsilon_0} \rho D (\nabla_x^3 G * \rho D), \\ \partial_t(\rho D) + \nabla_x \cdot (\rho D \otimes U + P^{dv}) + (\rho \Omega D + P^{d\omega})^\perp &= 0, \\ \partial_t(\rho \Omega) + \nabla_x \cdot (\rho \Omega U + P^{\omega v}) &= -\frac{1}{\epsilon_0} \rho D (\nabla_x^2 G * \rho D).\end{aligned}$$

with four pressure terms

$$\begin{aligned}P^{vv}(t, x) &:= \int_{\tilde{\mathbf{Z}}} (v - U) \otimes (v - U) f(t, x, \tilde{\mathbf{Z}}) d\tilde{\mathbf{Z}}, \\ P^{dv}(t, x) &:= \int_{\tilde{\mathbf{Z}}} (d(\theta) - D) \otimes (v - U) f(t, x, \tilde{\mathbf{Z}}) d\tilde{\mathbf{Z}}, \\ P^{d\omega}(t, x) &:= \int_{\tilde{\mathbf{Z}}} (\omega - \Omega)(d - D) f d\tilde{\mathbf{Z}}, \\ P^{\omega v} &= \int_{\tilde{\mathbf{Z}}} (\omega - \Omega)(v - U) f(t, x, \tilde{\mathbf{Z}}) d\tilde{\mathbf{Z}}.\end{aligned}$$

Return to BBGKY Hierarchy

To recover correlation in the continuum, return to the first-marginal in BBGKY. Introduce the second marginal residual

$$h_2(Z_1, Z_2) = f_2(Z_1, Z_2) - \overbrace{f_1(Z_1)f_1(Z_2)}^{f_1^{\otimes 2}}.$$

Rewrite the first marginal evolution as a Vlasov system “perturbed” by correlation

$$\boxed{\partial_t f_1 + V_1 \cdot \nabla_{X_1} f_1 + \nabla_{V_1} \cdot ((\mathbb{F} * f_1) f_1) = \mathcal{C}(h_2).}$$

Here $\mathbb{F} = (F^x, F^\theta)$, and the correlation term

$$\begin{aligned} \mathcal{C}(h_2) = & -\frac{\ell^2}{\epsilon_0} d(\theta_1) \int \nabla_x^3 G(x_1 - x_2) d(\theta_2) \nabla_{v_1} h_2 dZ_2 - \\ & \frac{1}{\epsilon_0} d(\theta_1) \int \nabla_x^2 G(x_1 - x_2) d(\theta_2) \nabla_{\omega_1} h_2 dZ_2. \end{aligned}$$

Hydrodynamic First Marginal

Take the moment projections against $\{1, v_1, \theta_1, \omega_1\}$ yields the same system given by the Vlasov but subject to additional, “stochastic” terms arising from the second marginal residual.

$$\begin{aligned}
 \partial_t \rho + \nabla_x \cdot (\rho U) &= 0, \\
 \partial_t(\rho U) + \nabla_x \cdot (\rho U \otimes U + P^{vv}) &= -\frac{\ell^2}{\epsilon_0} \left(\rho D (\nabla_x^3 G * \rho D) \right. \\
 &\quad \left. + \nabla_x^3 G \otimes_{12} : D_2 \right), \\
 \partial_t(\rho D) + \nabla_x \cdot (\rho D \otimes U + P^{dv}) + (\rho \Omega D + P^{d\omega})^\perp &= 0, \\
 \partial_t(\rho \Omega) + \nabla_x \cdot (\rho \Omega U + P^{\omega v}) &= -\frac{1}{\epsilon_0} \left(\rho D (\nabla_x^2 G * \rho D) \right. \\
 &\quad \left. + \nabla_x^2 G \otimes_{12} : D_2 \right).
 \end{aligned}$$

Here the two-marginal residual matrix displacement $D_2 : \mathbb{R}^4 \mapsto \mathbb{R}^{2 \times 2}$,

$$D_2(x_1, x_2, t) := \int_{\mathbb{R}^8} d(\theta_1) \otimes d(\theta_2) \boxed{\boxed{h_2(x_1, x_2, \tilde{z}_1, \tilde{z}_2)}} d\tilde{z}_1 d\tilde{z}_2.$$

Three-body Interaction Models

A water-ring memetic energy on $X = (x_1, \dots, x_N)$ particles with interparticle distances $\ell_{ij} = |x_i - x_j|$ uses the potential energy

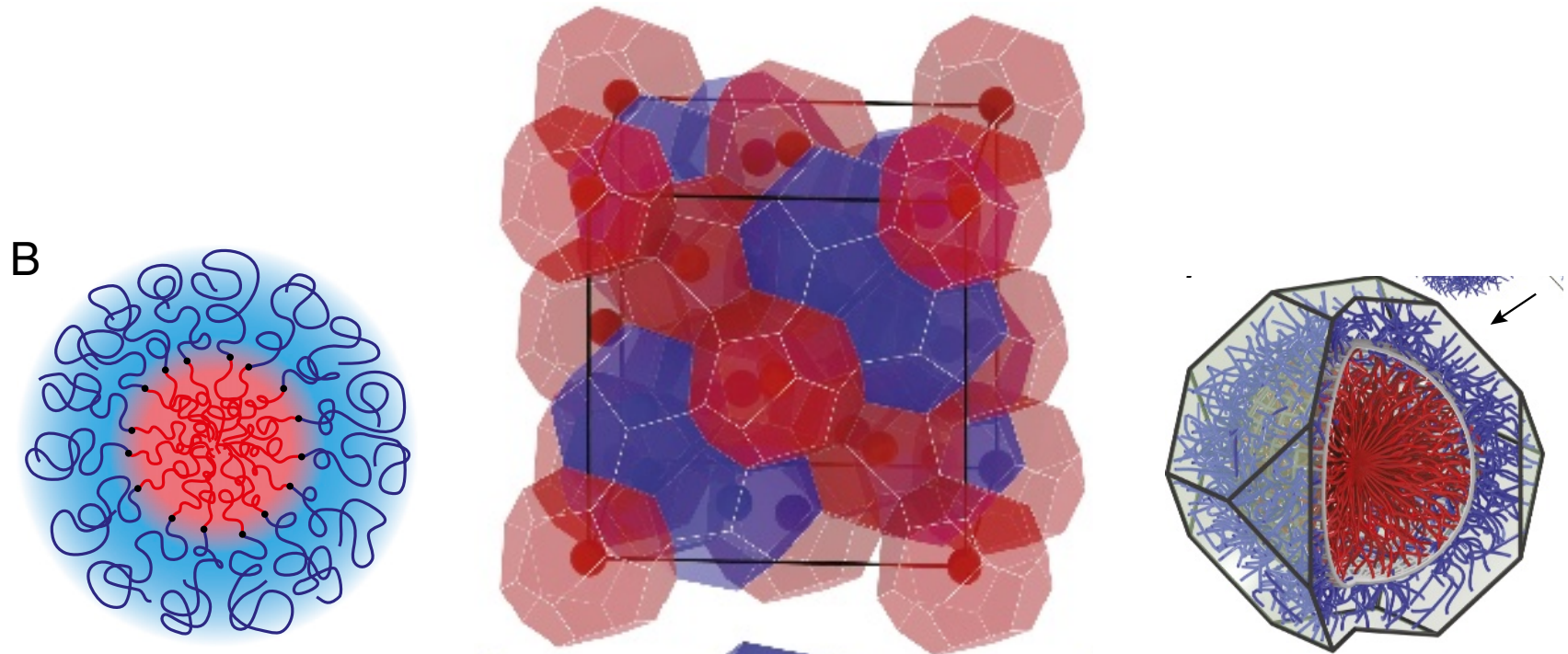
$$\mathcal{U}(X) = \sum_{i \neq j \neq k}^N \frac{(\ell_{ij} - \ell_{ik})^2 + (\ell_{ij} - \ell_{jk})^2 + (\ell_{ik} - \ell_{jk})^2}{e^{(\ell_{ij}^2 + \ell_{jk}^2 + \ell_{ik}^2)/\ell^2}}.$$

This simple three-body energy penalizes variation in the separation distance of **near-neighbors**.



Getty Villa Peristyle

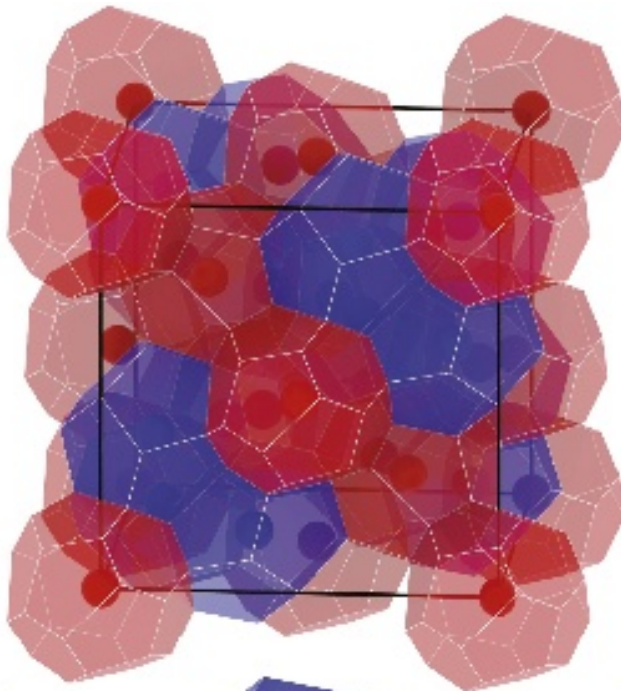
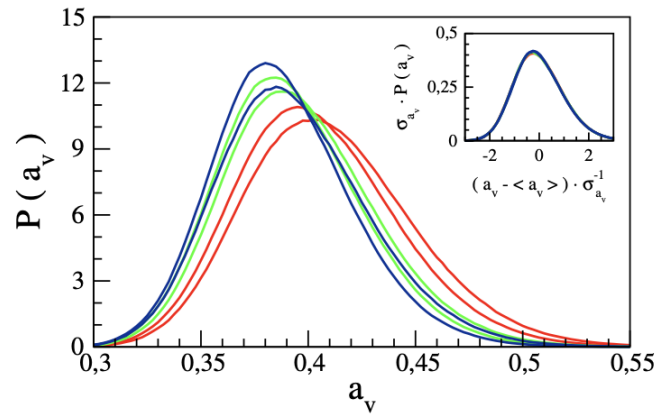
Packing by Spherical Micelles



Reddey et al PNAS 2018

Some amphiphilic diblocks in solvent form spherical micelles. When “over-packed” they arrange into space filling patterns resembling dodecagonal quasicrystals including regions of different volumes.

Voronoi Metrics of Water



Molecular positions generate a Voronoi partition of domain. Asphericity:

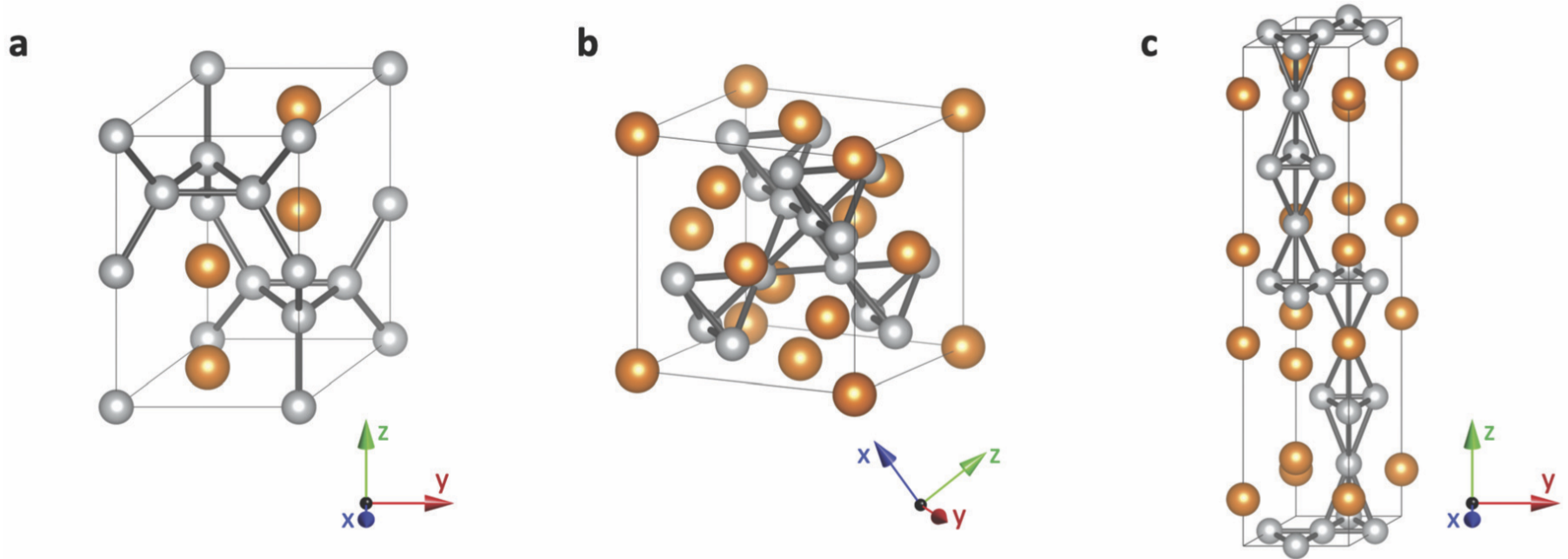
$$a_v := \frac{S^3}{36\pi V^2} - 1 > 0$$

can characterize distribution.

For glassy systems near glass transition point asphericity has universal deviation about mean: Bermini et al J. Non-Crystalline Solids (2015).

Gradient flow on asphericity yields optimal arrangements of dodecagonal quasicrystals including regions of different volumes. Reddey et al PNAS 2018.

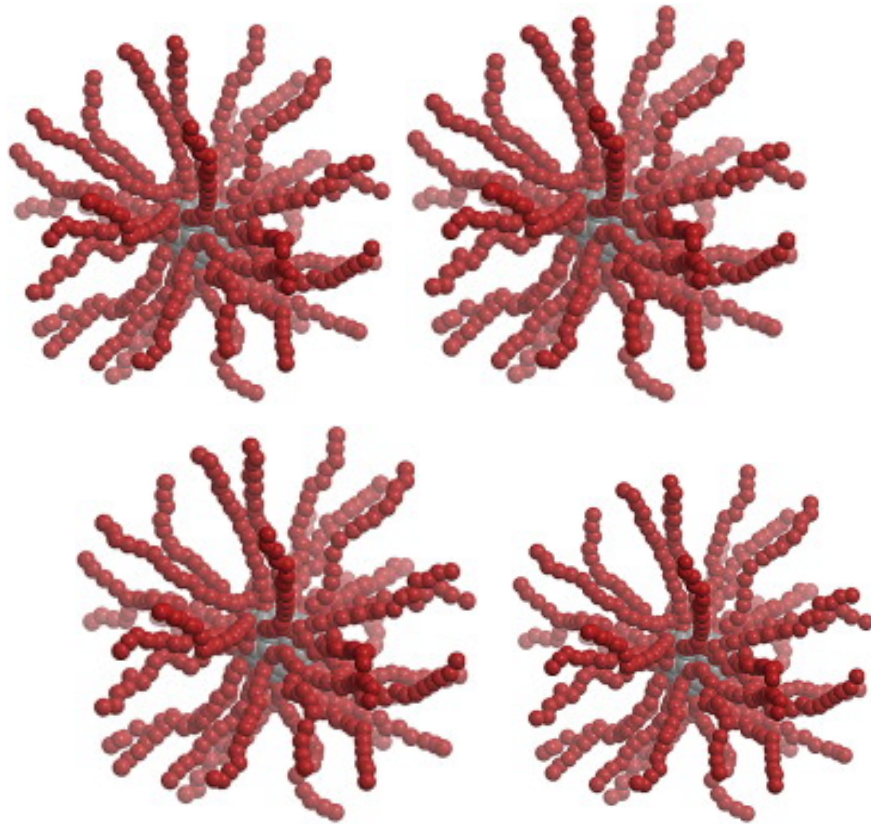
Periodic “Laves Phases”



Dorfman - Soft Matter (2021). Careful numerical analysis on models derived from self-consistent mean field theory suggests existence of periodic “Laves Phases” with 15, 18 and 38 repeat units. These require careful tuning of the aspect ratio of the computational domain.

Star Polymers: A Model System

As a model system Frank Bates confined star-polymers and introduced a simplified asphericity energy based upon Voronoi diagrams



The Hookean-Voronoi Energy: Kenny Jao & Sam Sottile

Place N sites

$$\mathbf{x} := (\vec{x}_1, \dots, \vec{x}_N) \in \mathbb{R}^{2N},$$

in a rectangle

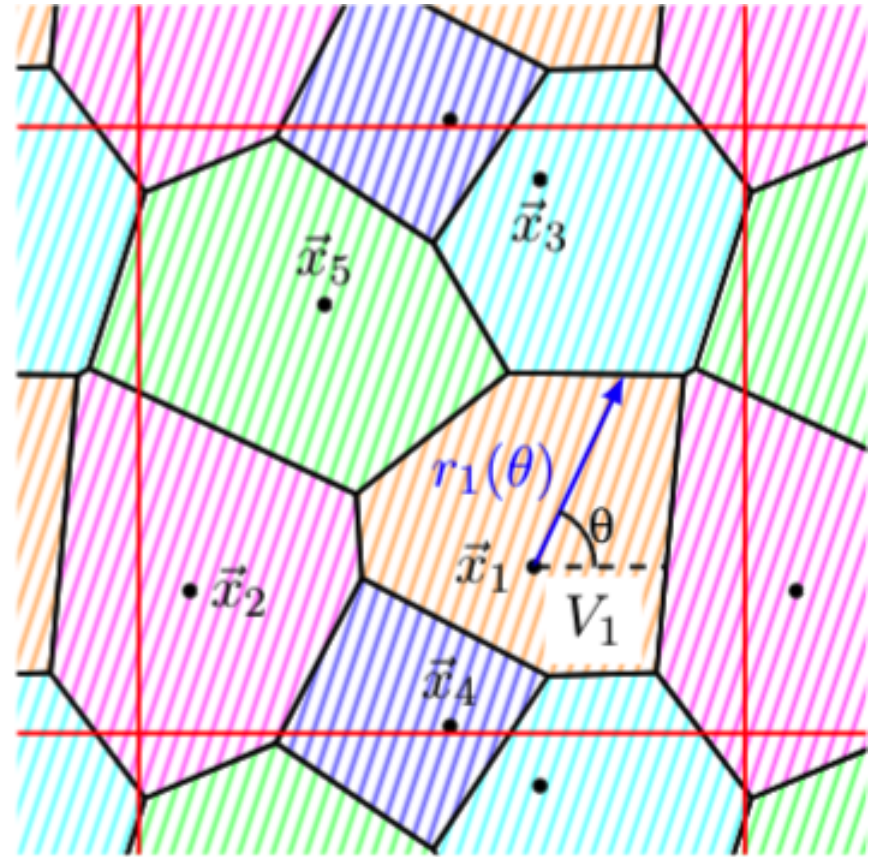
$$\Omega_\alpha = [0, \sqrt{\alpha N}] \times \left[0, \sqrt{\frac{N}{\alpha}}\right],$$

of area N and aspect ratio $\alpha \in (0, 1]$.

Form the Ω_α periodic Voronoi diagram. In each Voronoi region V_i , calculate the simple Hookean energy

$$E_i(\mathbf{x}) := \int_0^{2\pi} |r_i(\theta) - r_*|^2 d\theta.$$

Here r_i is distance from site x_i to ∂V_i at angle θ , and r_* is equilibrium chain length.



Average Radius of a Convex Domain

The average radius of the Voronoi region V_i with respect to $\vec{x}_i \in V_i$,

$$\bar{r}_i := \frac{1}{2\pi} \int_0^{2\pi} r_i(\theta) d\theta,$$

The Hookean-Voronoi energy

$$E(\mathbf{x}) := \sum_{i=1}^N E_i(\mathbf{x}),$$

can be expressed as

$$\begin{aligned} E(\mathbf{x}) &= \sum_{i=1}^N \int_0^{2\pi} (r_i^2(\theta) - 2r_* r_i(\theta) + r_*^2) d\theta, \\ &= \sum_{i=1}^N (2|V_i| - 4\pi r_* \bar{r}_i + 2\pi r_*^2), \\ &= \textcolor{blue}{C(N)} - 4\pi r_* \sum_{i=1}^N \bar{r}_i(\mathbf{x}). \end{aligned}$$

Minimize Hookean-Voronoi energy by maximizing average radii.

For Fun

Reverse Isoparametric Inequality: For any convex domain V and any $x \in V$

$$\pi \bar{r}^2(x) \leq |V|.$$

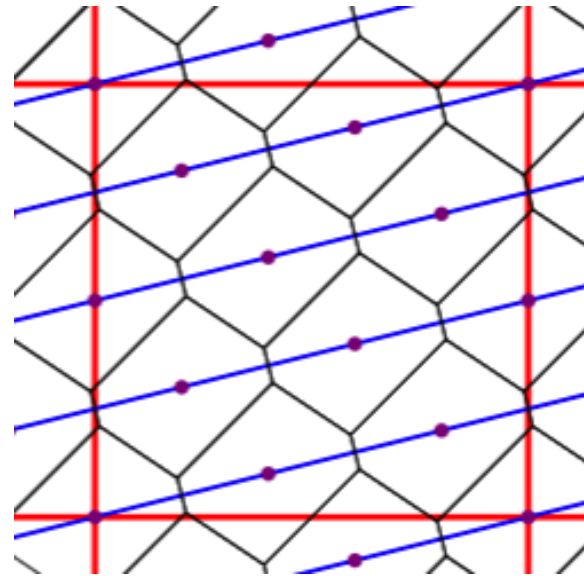
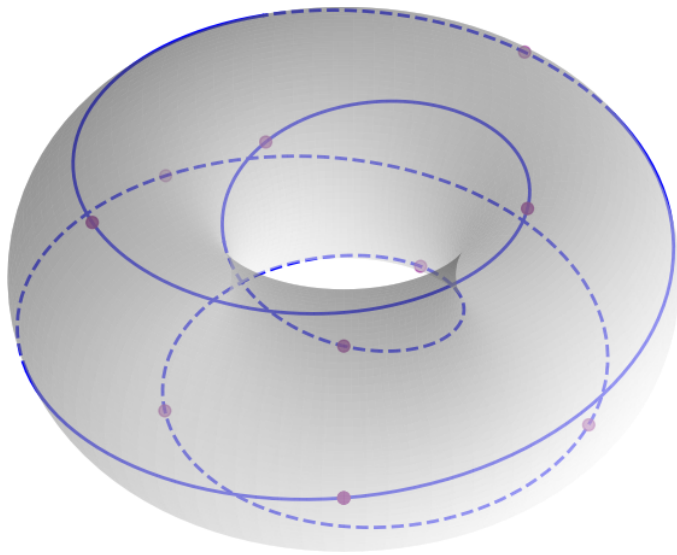
Proof: Jensen's inequality with convex function $s \mapsto s^2$,

$$\bar{r}^2 = \left(\frac{1}{2\pi} \int_0^{2\pi} r(\theta) \, d\theta \right)^2 \leq \frac{1}{2\pi} \int_0^{2\pi} r^2(\theta) \, d\theta = \frac{|V|}{\pi}.$$

Single-String Ordered States

A tessellation is ordered if all regions are isometric, otherwise disordered.

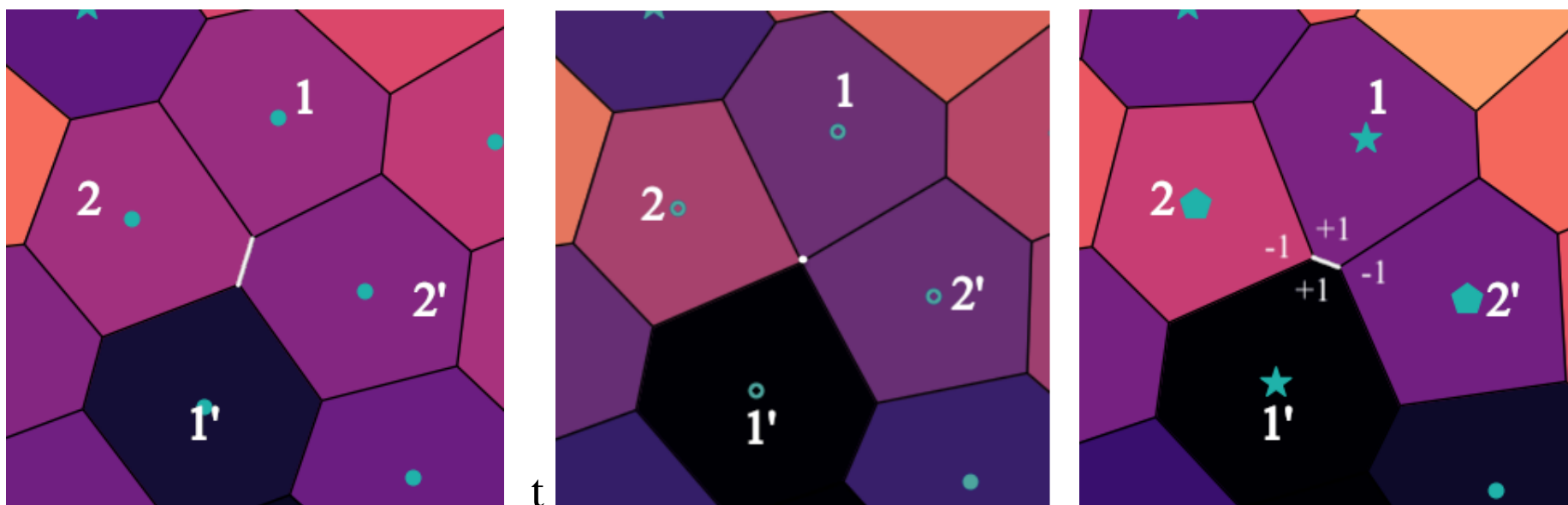
The string construction: wrap a line around torus with slope that results in a closed curve. Place N equally spaced sites on the closed line – these form a Voronoi diagram with equal shapes.



This construction yields a finite number of ‘single-string’ ordered Voronoi tessellations. These are equilibria of E .

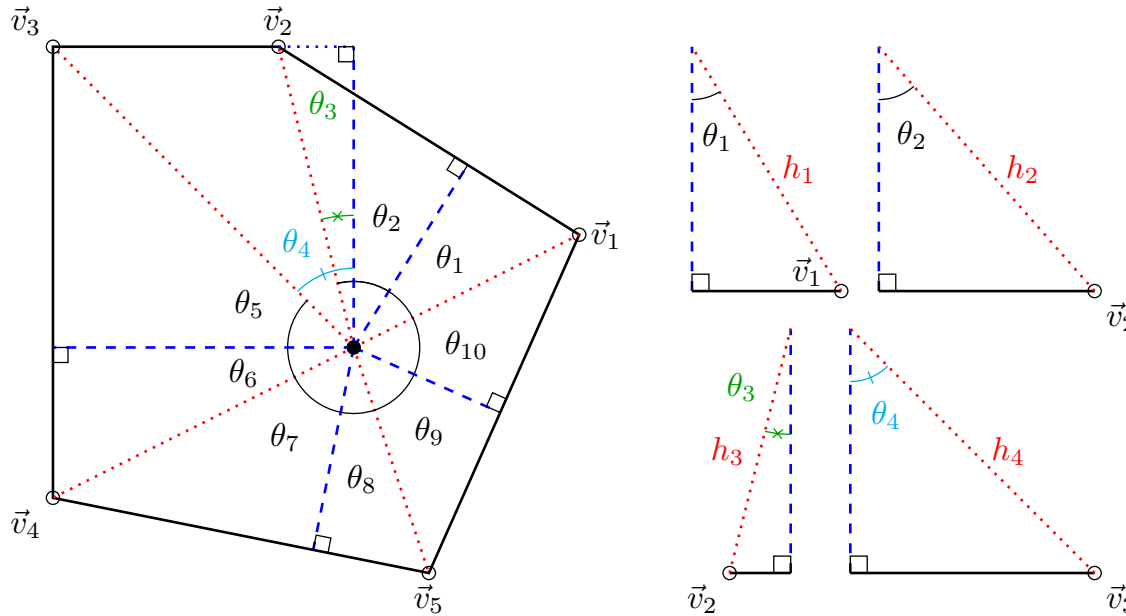
3-Body Interactions & Defect Bifurcations

The Voronoi cell is generically defined through 3-body interactions of “near-neighbors”



A generic Defect Bifurcation through vertex collision. Generates two pair of 5- and 7-sided **defect** regions from two pair of 6-sided regions.

Hexagonal Supremacy by Convexification



Cut each Voronoi region with m_i edges into $2m_i$ right triangles: total of $K \leq 12N$ (Euler's formula) triangles.

Maximize average radius subject to two constraints on interior angle sum and total area

Reduced problem has almost no geometric constraints – it is convex for each value of K and the global maximum is achieved at $K = 12N$, when the triangles are the 12 pieces of the hexagon.

$$\sum_{i=1}^K \theta_i = 2\pi N,$$

$$\sum_{i=1}^K \frac{1}{2} h_k \sin \theta_k = N.$$

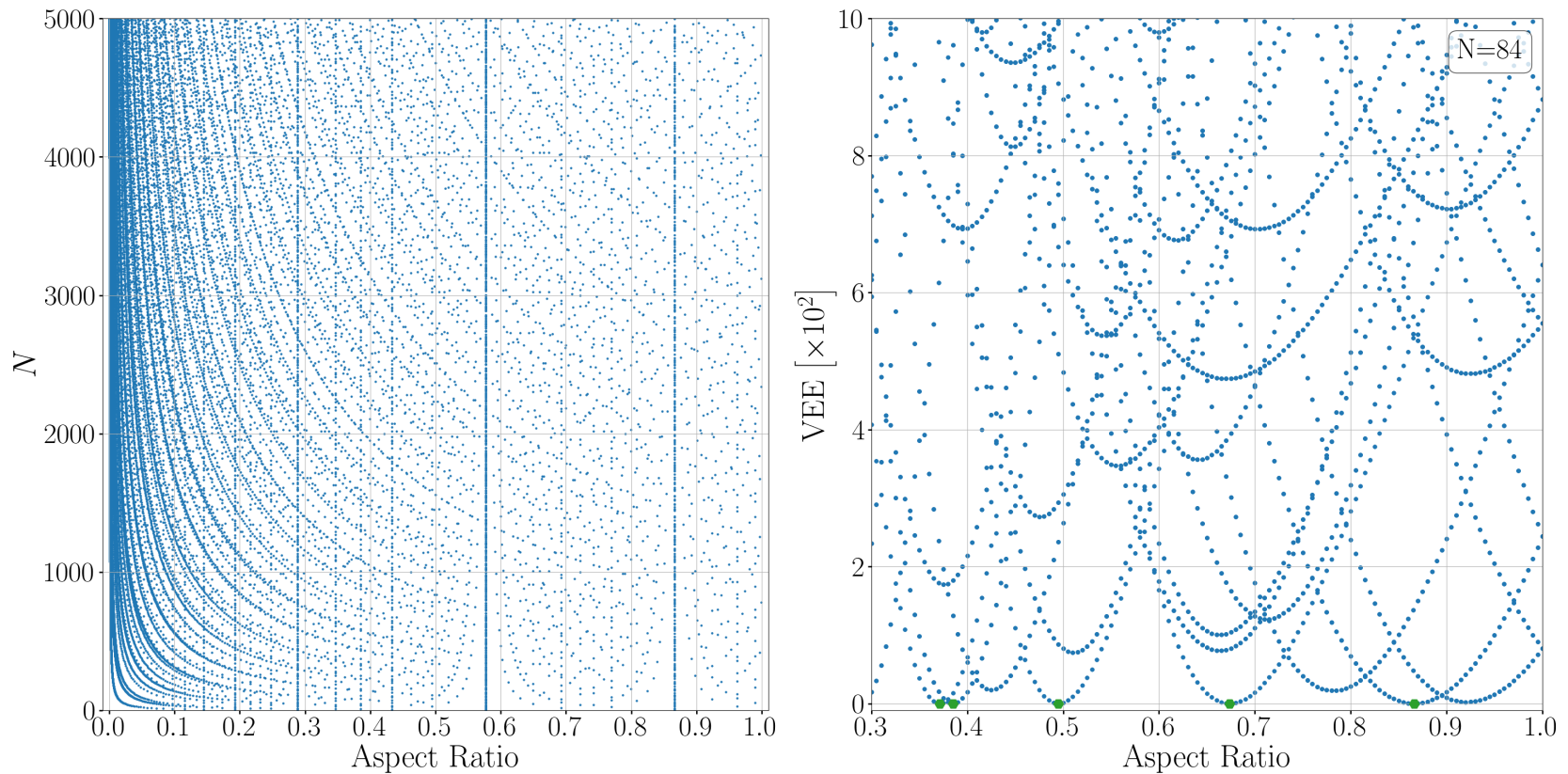
If the Hexagonal pieces tile Ω_α then its the minimizer.

Regular Hexagonal and Ordered Equilibria

Introduce the volume averaged excess energy

$$\overline{E}(\mathbf{x}) := \frac{E(\mathbf{x})}{N} - E_{\text{hex}} \geq 0.$$

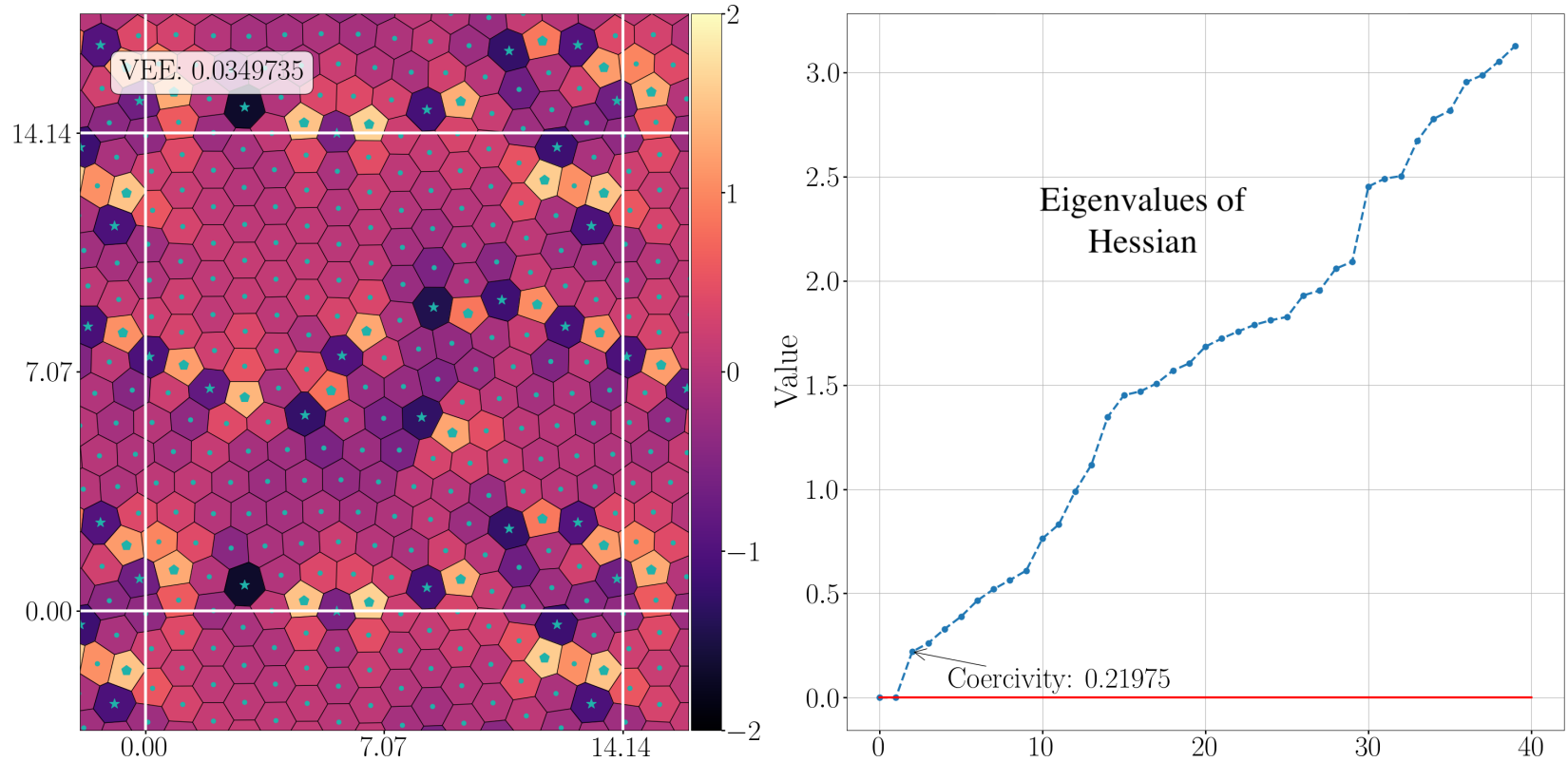
For which N and α is the regular hexagon achieved?



Gradient Flow



Equilibria of the Gradient Flow

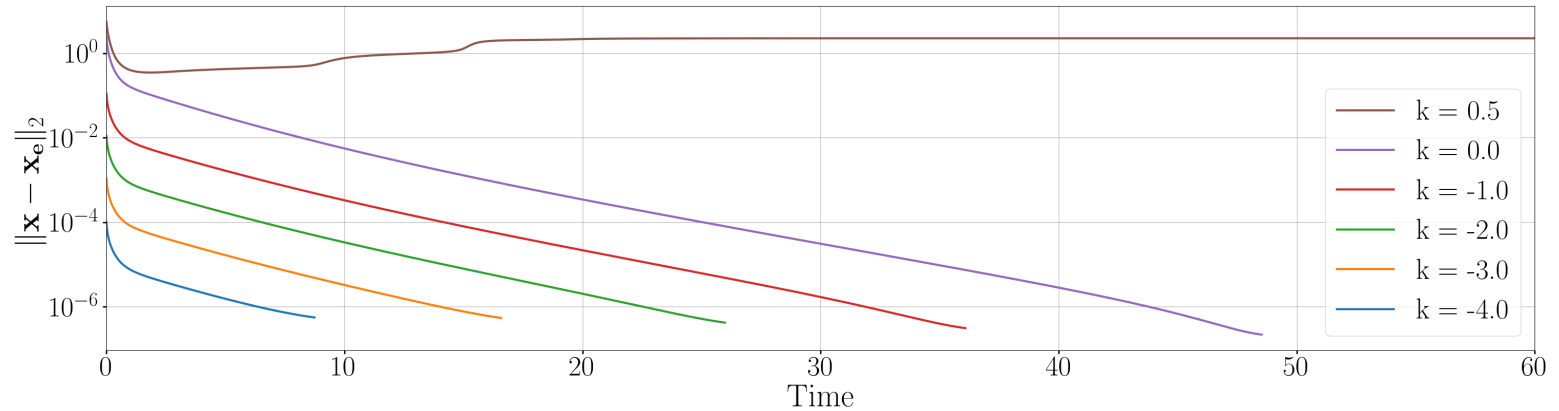


Defects: Non-six sided Voronoi regions – generically 5-7 pairs.

Stopping Condition: $\nu(\mathbf{x}_{\text{eq}})$ smallest nonzero eigenvalue of $\nabla^2 \bar{E}(\mathbf{x}_{\text{eq}})$,

$$\frac{\|D_{\mathbf{x}} \bar{E}(\mathbf{x}_{\text{eq}})\|_2}{\nu(\mathbf{x}_{\text{eq}})} \leq \delta_{\text{eq}} = 10^{-5}.$$

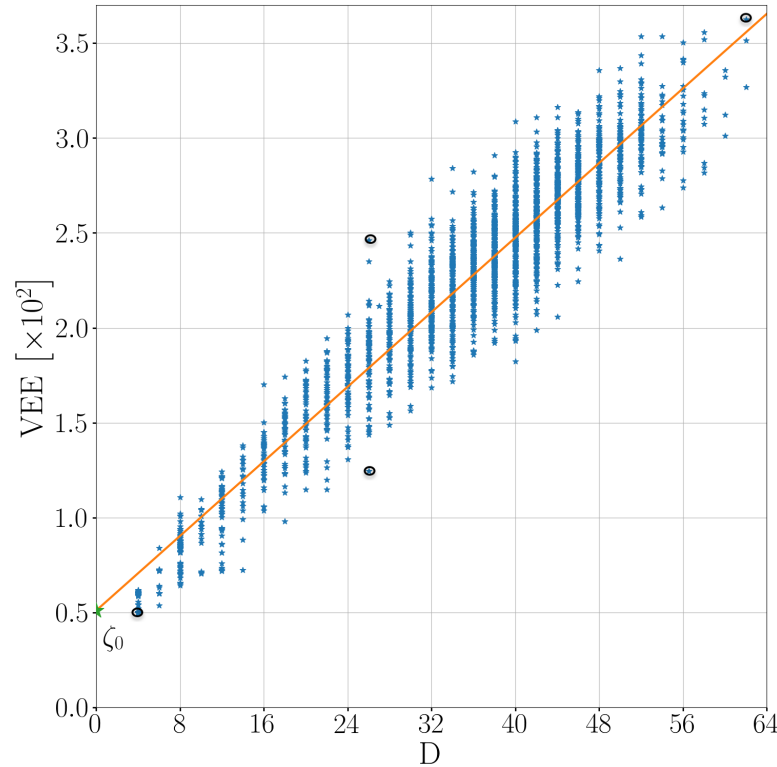
Prodigal Equilibria



Evolution of $\|x(t) - x_{eq}\|_2$ following perturbation of x_{eq} of size 10^k for $k = -4, -3, -2, -1, 0, 0.5$. Return to x_{eq} at fixed exponential rate, except for largest perturbation.

Large N and Frustration

Frustration refers to the inability of a system to arrive at its ground state energy.



$\mathcal{B}(400, 1, 2500)$

Linear fit to \bar{E} verses defect number D
 $\bar{E} \approx \zeta_0 + \zeta_1 D.$

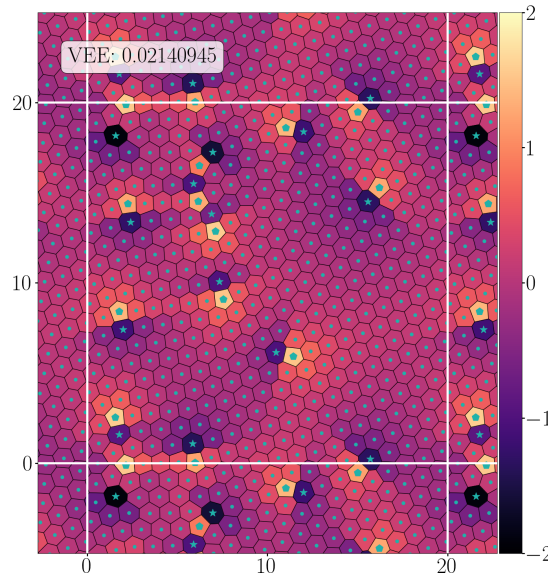
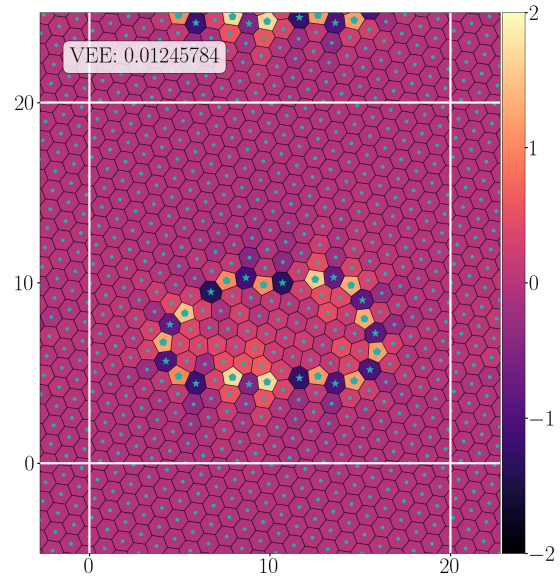
Define *frustration* \mathcal{F} of a bin $\mathcal{B}(N, \alpha, S)$ as the product

$$\mathcal{F}(\mathcal{B}(N, \alpha, S)) = \zeta_1(N, \alpha) \langle D \rangle_{\mathcal{B}}.$$

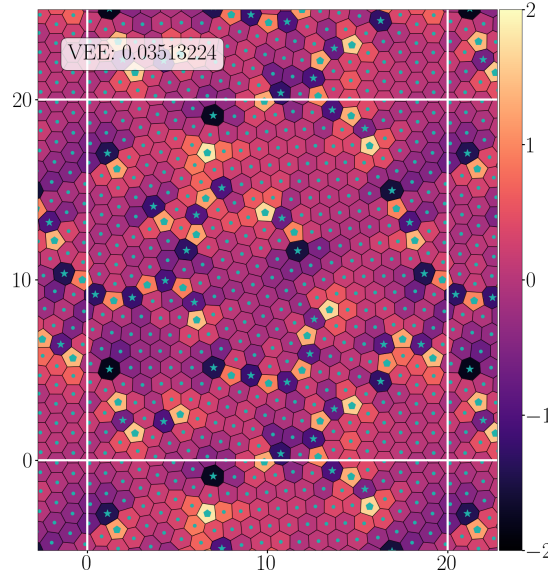
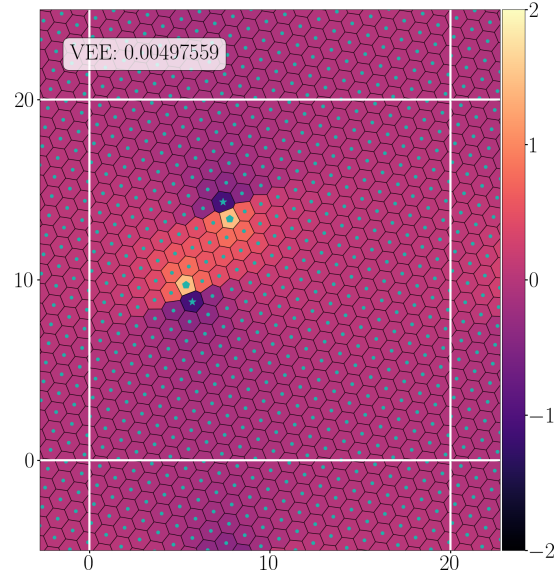
The frustration is the contribution of defects, per Voronoi domain, to $\langle \bar{E} \rangle_{\mathcal{B}}$ that the gradient flow is unable to eliminate

$$\langle \bar{E} \rangle_{\mathcal{B}} = \zeta_0 + \mathcal{F}.$$

$N = 400$, Equilibria with Defects

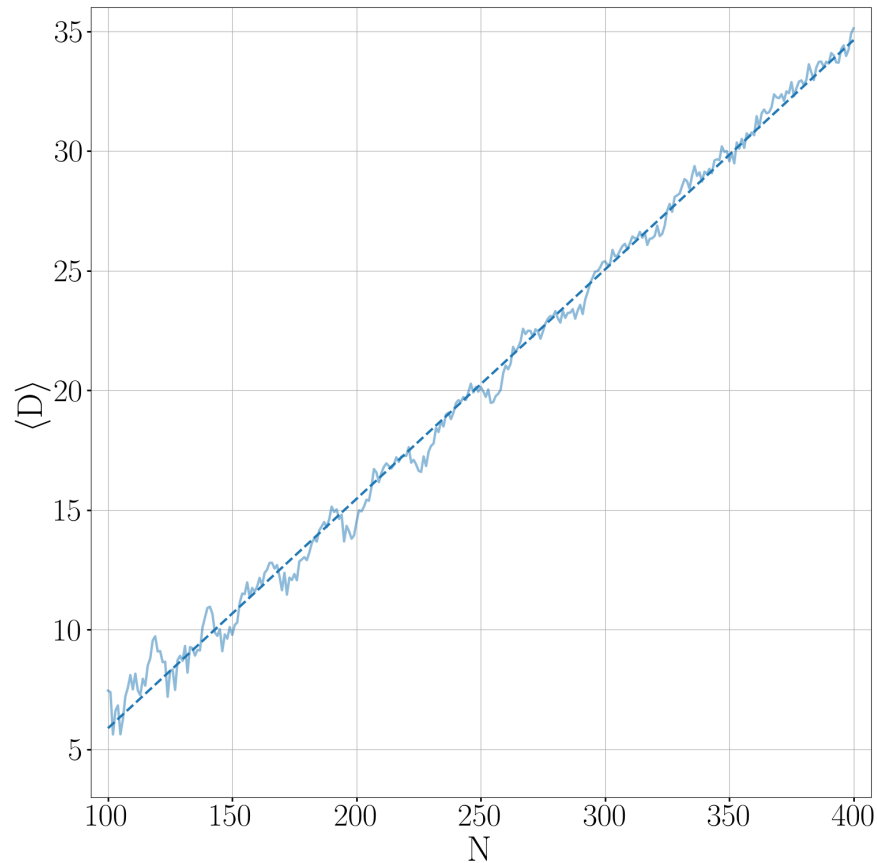


Equilibria with 26 defects,
equal to 6.5% of cells



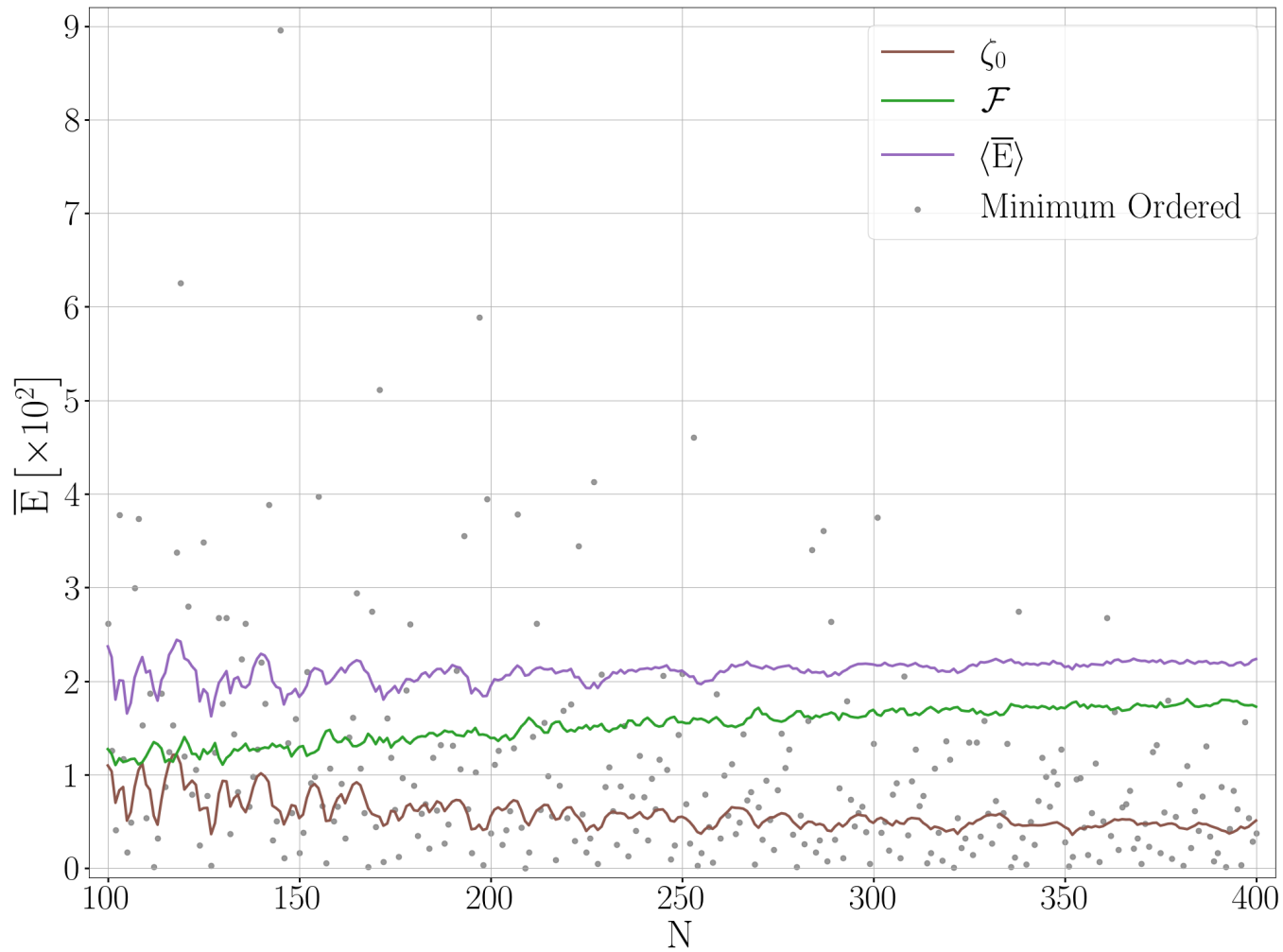
Equilibria with 4 & 62 de-
fects,
equal to 1% and 15.5% of
cells.

Large N limits: Defects



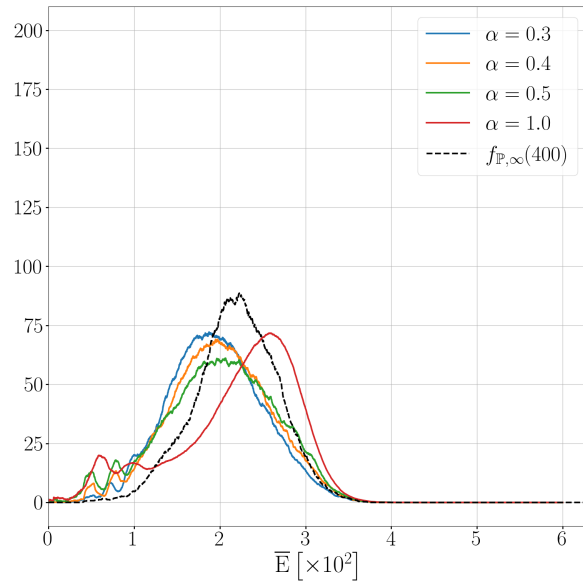
For $\alpha = 1$, the average defects $\langle D \rangle_{\mathcal{B}}$, computed from $\mathcal{B}(N, 1, 2500)$ for $N = 100, \dots, 400$. The best linear fit to $\langle D \rangle_{\mathcal{B}(N)}$ for $N \geq 100$ has slope $\eta_1(1) \approx 0.088$.

Large N limits

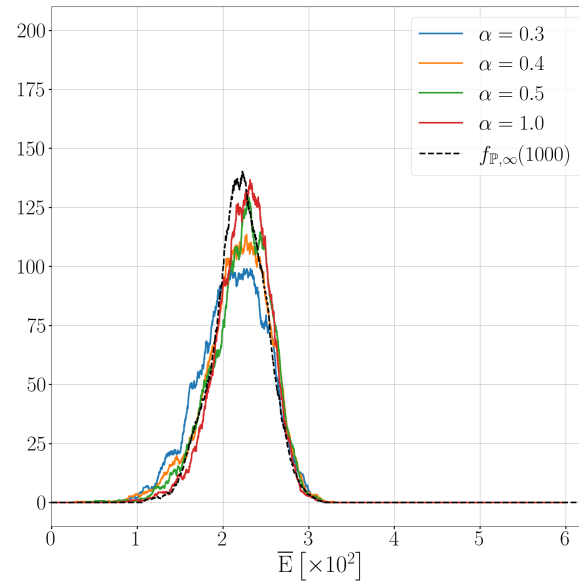


The average $\langle \bar{E} \rangle_{\mathcal{B}(N,1,2500)}$ decomposed into the ground state $\zeta_0(N, 1)$ and the frustration $\mathcal{F}(N, 1)$. **Minimum ordered energy does not correlate to ζ_0 .**

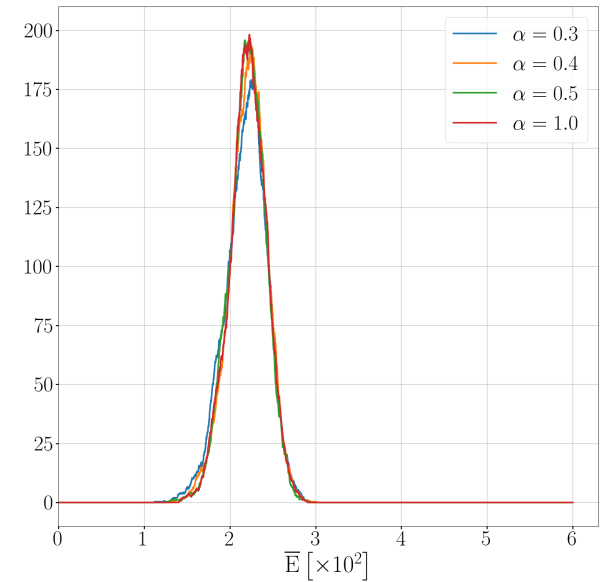
Large N and the Universal Measure \mathbb{P}



$N = 400$



$N = 1000$



$N = 2000$

Probability densities for limiting energy from random initial data.

Suggests $N \rightarrow \infty$ convergence to a δ -function distribution

$$f_{\mathbb{P},\infty}(\bar{E}; N) := \sqrt{N} f_{\mathbb{P},*} \left(\frac{\bar{E} - \bar{E}_*}{\sqrt{N}} \right) \rightarrow \delta_{\bar{E}_*}.$$

Conjecture: non-zero limiting bulk frustration $\bar{E}_* > 0$.

Jao, P., Sottile, **Physica D** (2023)

Mean-Field Limits in Multi-body Interactions

In a mixed two and three body Hamiltonian flow

$$\begin{aligned}\frac{d}{dt}x_i &= v_i, \\ \frac{d}{dt}v_i &= \frac{1}{N} \sum_{j=1}^N F_2(x_i, x_j) + \frac{1}{N^2} \sum_{j=1}^N \sum_{k=1}^N F_3(x_i, x_j, x_k),\end{aligned}$$

then a mean field limit for the pdf f takes the form

$$f_t + v \cdot \nabla_x f + \nabla_v \cdot \left(\left(\int_{\mathbb{R}^d} F_2(x_1, x_2) f(x_2) dx_2 + \int_{\mathbb{R}^{2d}} F_3(x_1, x_2, x_3) f(x_2) f(x_3) dx_2 dx_3 \right) f \right) = 0.$$

This does not seem fundamentally different, but the point may be that the mean field does not hold.

Acknowledgments



NSF-DMS 1813203
NSF-DMS 2205553

